Significance of Pressure Drop, Changing Molar Flow, and Formation of Steam in the Accurate Modeling of a Multi–Tubular Fischer–Tropsch Reactor with Cobalt as Catalyst

Christoph Kern, Andreas Jess* (jess@uni-bayreuth.de)

Supporting Information

Supplement to Chapter 2.2: Equations of two-dimensional model of a tube of a FT-reactor

The rearrangement of the Eqs. (8) and (9) (see main text) lead to the following mass and heat balances (Eqs. (S1) and (S2)).

Mass balances for component i

(R1: formation of CH_4; R2: formation of C_{2+}-hydrocarbons):

$$u_s \frac{dc_i}{dz} = -c_i \frac{du_s}{dz} + \left(\nu_{i,R1}\, r_{m,CO,R1,eff} + \nu_{i,R2}\, r_{m,CO,R2,eff}\right)\rho_{bed} \quad \text{(S1)}$$

with $\nu_{CO,R1} = -1;\ \nu_{H2,R1} = -3;\ \nu_{CH4,R1} = 1;\ \nu_{H2O,R1} = 1$

$\nu_{CO,R2} = -1;\ \nu_{H2,R2} = -2;\ \nu_{CH2+,R2} = 0.13;\ \nu_{H2O,R2} = 1$

Remark on the mass balance for the production of C_{2+}-HCs: For a chain growth probability of FTS for C_{2+}-HCs of 0.85 [3], 92 wt.-% of the C_{2+}-HCs have C-numbers of 2 to 25, assumed to be completely in the gas phase (for the conditions of a total pressure of 30 bar and 230°C as mean reaction temperature). The average C-number of the gaseous C_{2+}-HCs with 2 to 25 carbon atoms, is about 8. Hence, each mol CO converted into C_{2+}-HCs leads to 0.13 mol of C_{2+}-HCs in the gas phase.

Heat balance:

$$u_s \frac{dT}{dz} = -T \frac{du_s}{dz} + \frac{\lambda_{rad}}{c_p\, c_g} \frac{1}{r} \frac{dT}{dr} + \frac{\lambda_{rad}}{c_p\, c_g} \frac{d^2T}{dr^2} + \left(r_{m,CO,R1,eff}(-\Delta_R H_{R1}) + r_{m,CO,R2,eff}(-\Delta_R H_{R2})\right) \frac{\rho_{bed}}{c_p\, c_g} \quad \text{(S2)}$$

Change of superficial gas velocity u_s in volume element *dV* and differential length *dz*:

Ideal gas law leads to the differential change of the volume rate:

$$\frac{d\dot{V}_g}{dV} = \frac{d\left(\dot{n}_{total}\, R\, T / p_{total}\right)}{dV} = \frac{du_s}{dz} \quad \text{(S3)}$$

The differential change of u_s in axial direction, Eq. (S4), is the result of a) the decreasing total molar flow rate by the methanation and the FT reaction, Eq. (S5), b) the change of the (radial mean) temperature, Eq. (S6), and c) the pressure drop, Eq. (S8):

$$\frac{du_s}{dz} = \frac{d\left(\dot{n}_{total}\, R\, T / p_{total}\right)}{dV} = \frac{R\,T}{p_{total}} \frac{d\dot{n}_{total}}{dV} + \frac{\dot{n}_{total}\, R}{p_{total}} \frac{dT}{dV} + \dot{n}_{total}\, R\, T \frac{d\left(1/p_{total}\right)}{dV} \quad \text{(S4)}$$

a) The change of the total molar flow rate $d\dot{n}_{total}$ depends on the change (here decline) of the total number of moles present in the gas phase by the methanation reaction ($\Delta_{R1}\nu_i$)

and by the FT reaction ($\Delta_{R2}\nu_i$). This leads to the following equation for the change of the gas velocity due to both reaction:

$$\left.\frac{du_s}{dz}\right|_{T,p} = \frac{R\,T}{p_{total}}\frac{d\dot{n}_{total}}{dV} = \frac{\rho_{bed}}{c_g}\left(\Delta_{R1}\nu_i\ r_{m,CO,R1,eff} + \Delta_{R2}\nu_i\ r_{m,CO,R2,eff}\right) \quad \text{(S5)}$$

with $\Delta_{R1}\nu_i = -2$ and $\Delta_{R2}\nu_i = -1.87$

b) The change of gas velocity u_s in a differential axial segment Δz is calculated from the difference between the temperature in the differential segment (n) and the temperature in the previous differential segment (n-1):

$$\left.\frac{du_s}{dz}\right|_{\dot{n},p} = \frac{\dot{n}_{total}\,R}{p_{total}}\frac{dT}{dV} = \frac{c_g\,A\,u_s\,R}{p_{total}}\frac{dT}{A\,dz} = \frac{c_g\,u_s\,R}{p_{total}}\frac{dT}{dz} = \frac{u_s}{T}\frac{\Delta T}{\Delta z}$$

$$= \frac{u_{s,n-1}}{T_{mean}}\frac{(T_{mean,n} - T_{mean,n-1})}{\Delta z} \quad \text{(S6)}$$

Whereby the radial mean temperature in the cylindrical tube (fixed bed) is given by:

$$T_{mean,bed} = \frac{\int_0^{r_t} T\ 2\,\pi r\,dr}{\pi\,r_t^2} \approx T\ at\ r = 0.7\ r_t \quad \text{(S7)}$$

c) Analogous to the temperature dependence, the change of u_s as a result of the change of total pressure is calculated from the difference between the pressure in the differential segment (n) and the pressure in the previous differential segment (n-1):

$$\left.\frac{du_s}{dz}\right|_{\dot{n},T} = \dot{n}_{total}\,R\,T\,\frac{d(1/p_{total})}{dV} = c_g\,A\,u_s\,R\,T\,\frac{d(1/p_{total})}{A\,dz} = p\,u_s\,\frac{\Delta(1/p_{total})}{\Delta z}$$

$$= p_{total}\,u_{s,n-1}\,\frac{1/p_{total,n} - 1/p_{total,n-1}}{\Delta z} \quad \text{(S8)}$$

For an axial segment n of the tubes (fixed bed) with length Δz the pressure drop $\Delta p_{bed,n}$ is given by the *Ergun* equation [8,15]:

$$\Delta p_{bed,n} = p_{total,n-1} - p_{total,n} = f_b\,\frac{\Delta z}{d_p}\,\frac{M_g\,c_g}{2}\,u_{s,n-1}^2 \quad \text{(S9)}$$

$$f_b = \frac{(1-\varepsilon_{bed})}{\varepsilon_{bed}^3}\left(3.5 + \frac{300\,(1-\varepsilon_{bed})}{Re_p}\right) \approx 33 + \frac{1700}{Re_p} \text{ (for spherical particles and } \varepsilon_p \approx 0.4) \quad \text{(S10)}$$

<u>Determination of the radial heat transfer from the fixed bed to the boiling water cooling</u>

The boundary condition at the inner wall of the tubes ($r = r_t$) with $T_{t,bed}$ as temperature of the fixed bed directly at the wall before a temperature jump (because of $\alpha_{w,int}$) occurs, is:

$$\lambda_{rad}\left.\frac{dT}{dr}\right|_{r\,=\,r_t} = k_d(T_{cool} - T_{r_{t,bed}}) \quad \text{(S11)}$$

The thermal transmittance (from inner wall of tube to boiling water), k_d, is thereby:

$$\frac{1}{k_d} = \frac{1}{\alpha_{W,int}} + \frac{\frac{d_{t,int}}{2}\ln\left(1+\frac{2\,s_{wall}}{d_{t,int}}\right)}{\lambda_{wall}} + \frac{\frac{d_{t,int}}{\left(d_{t,int}+2\,s_{wall}\right)}}{\alpha_{H_2O}} \quad \text{(S12)}$$

The effective radial thermal conductivity in the fixed bed ($Re_p = u_s\ d_p/\nu_g$; $Pr = \nu_g\ \rho_g\ c_p/\lambda_g$) is calculated by:[4-6]

$$\lambda_{rad} = \lambda_g \left\{ 4 + \frac{Re_p\ Pr}{7\left[2-\left(1-2\frac{d_p}{d_{t,int}}\right)^2\right]} \right\} \quad \text{(S13)}$$

The heat transfer coefficient at the inner tube wall $\alpha_{W,int}$ can be calculated by [8,11,12]

$$\alpha_{W,int} = \frac{\lambda_g}{d_p}\left[4\left(1.3 + 5\ \frac{d_p}{d_{t,int}}\right) + 0.19\ Re_P^{3/4} Pr^{1/3}\right] \quad \text{(S14)}$$

The heat transfer coefficient α_{H_2O} (external tube wall to boiling water; W m^{-2} s^{-1}) with $p_{H_2O,boil}$ in bar and $\dot{q}_{limit}$ in W m^{-2} is given by correlations based on literature data [8,12-14]:

$$\dot{q}_{limit} = 3780 - 48\ p_{H_2O,boil} \quad \text{(S15)}$$

with $p_{H_2O,boil} = \exp\left[12.5595 - \frac{4642.77}{(273+T_{cool})}\right]$ for 150°C < T_{cool} < 250°C (values listed in Tab. 7).

For $\dot{q}_{removal} < \dot{q}_{limit}$ (convection boiling): $\alpha_{H_2O} = 150\ \dot{q}_{removal}^{0.25}$ (S16)

For $\dot{q}_{removal} > \dot{q}_{limit}$ (nucleate boiling): $\alpha_{H_2O} = 2.03\ \dot{q}_{removal}^{0.7}\ p_{H_2O,boil}^{0.24}$ (S17)

A similar correlation as Eq. (S17) is given by Fritz [16], $\alpha_{H_2O} = 1.95\ \dot{q}_{removal}^{0.72}\ p_{H_2O,boil}^{0.24}$, which only leads to slightly higher results of α_{H_2O} (deviation = $\left|1 - 1.04\ \dot{q}_{removal}^{-0.02}\right|$ < 15%) for heat fluxes relevant for FT synthesis ($\dot{q}_{removal}$ < 10 kW m^{-2} s^{-1}).

The external heat transfer coefficient (including heat conduction through tube wall) $\alpha_{W,ex}$ is:

$$\frac{1}{\alpha_{W,ex}} = \frac{\frac{d_{t,int}}{2}\ln\left(1+\frac{2\,s_{wall}}{d_{t,int}}\right)}{\lambda_{wall}} + \frac{\frac{d_{t,int}}{\left(d_{t,int}+2\,s_{wall}\right)}}{\alpha_{H_2O}} = R_{th,ex,total} = R_{th,wall} + R_{th,H_2O} \quad \text{(S18)}$$

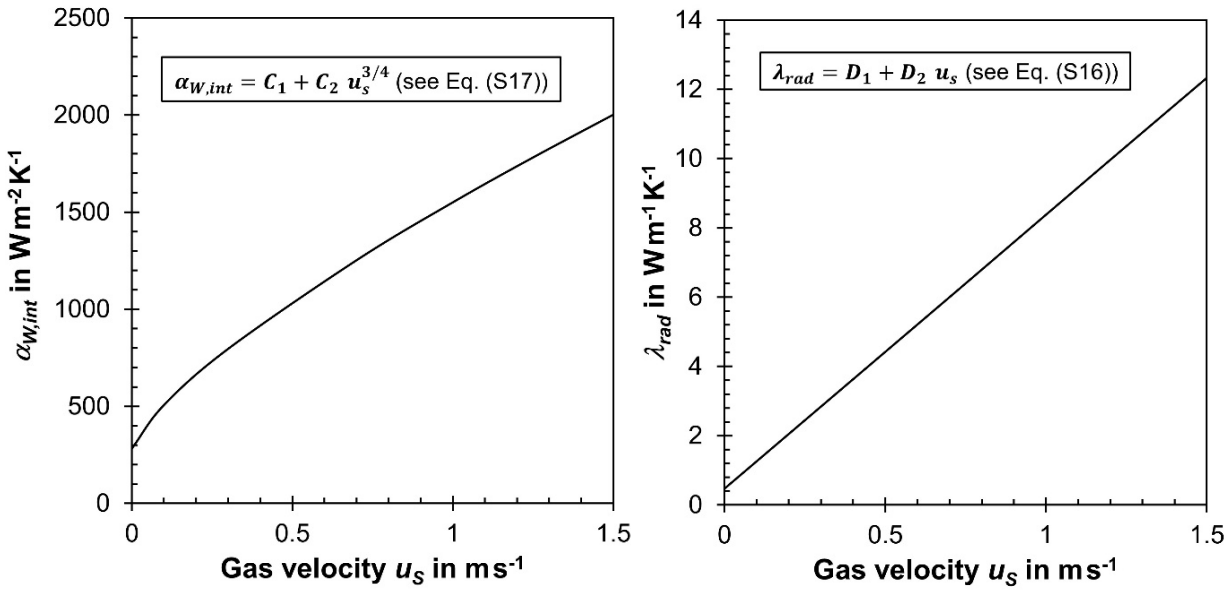

Fig. S1: Influence of superficial gas velocity on the heat transfer parameters λ_{rad} and $\alpha_{w,int}$ (230°C, p_{total} = 30 bar; 20% CO, 44% H_2, 36% CH_4).

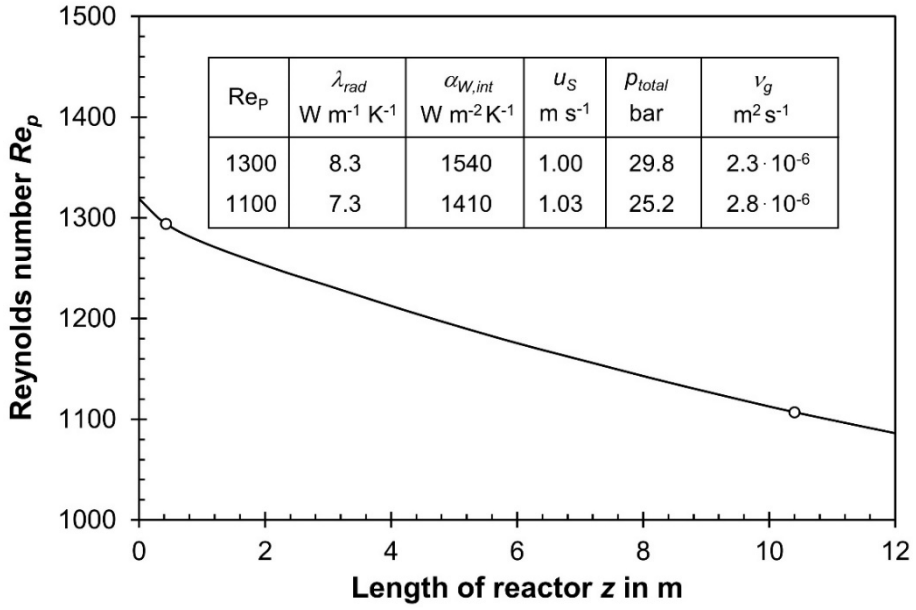

Re_P	λ_{rad} W m^{-1} K^{-1}	$\alpha_{W,int}$ W m^{-2} K^{-1}	u_S m s^{-1}	p_{total} bar	ν_g m^2 s^{-1}
1300	8.3	1540	1.00	29.8	$2.3 \cdot 10^{-6}$
1100	7.3	1410	1.03	25.2	$2.8 \cdot 10^{-6}$

Fig. S2: Axial profile of Reynolds number Re_p in the tubes of a multi-tubular FT reactor (model M3) and values of λ_{rad}, $\alpha_{w,int}$, u_s, p_{total}, and ν_g for two selected values of Re_p. Conditions: C_a = 3; $u_{s,\,z\,=\,0}$ (230°C, 30 bar) = 1 m/s; p_{total} = 30 bar; $X_{CO,total}$ = 95%; S_{CH_4} = 20%; molar H_2-to-CO ratio = 2.2; T_{max} = 240°C.

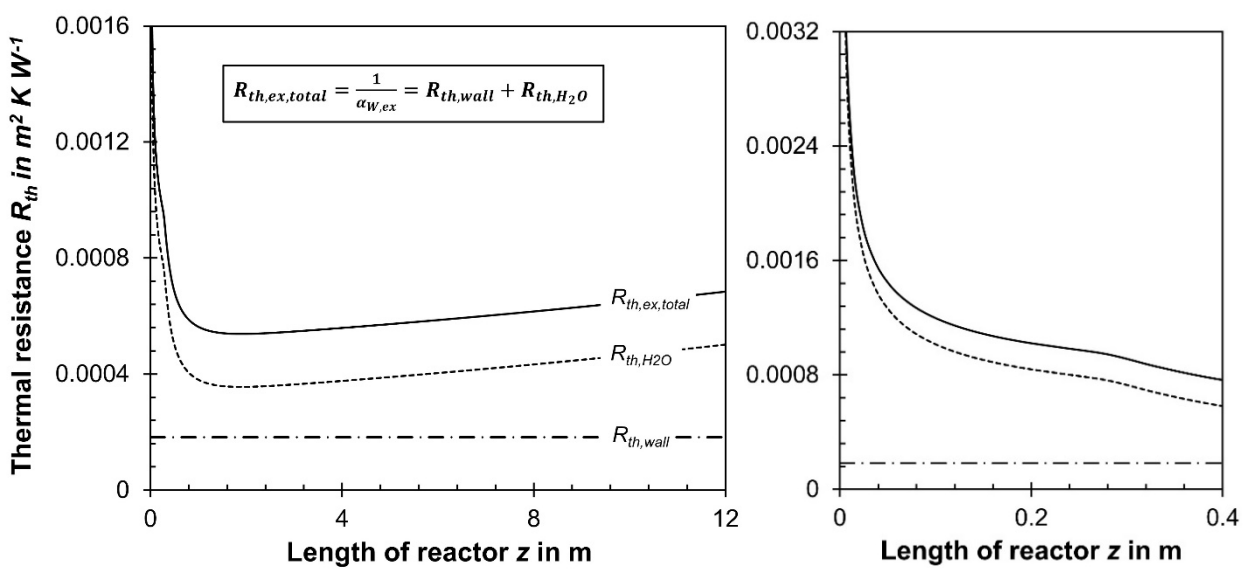

Fig. S3: Profiles of thermal resistance of tube wall and external heat transfer to boiling water ($R_{th,ex,total}$), and individual contributions of wall ($R_{th,wall}$) and external heat transfer alone ($R_{th,H2O}$) as calculated by all models except M0, see Eq. (S18) (conditions in Fig. 1).

Note that the overall thermal resistance, which also includes the heat transfer in the bed ($R_{bed} \approx 0.25\ d_{t,int}/\lambda_{rad}$) and at the internal wall ($R_{w,int} = 1/\alpha_{w,int}$), i.e. $R_{overall} = R_{bed} + R_{w,int} + R_{th,ex,total}$) is around 0.0022 m² K W⁻¹. $R_{overall}$ is almost constant along the tubes and corresponds to an overall thermal transmittance of about 460 W m⁻¹ K⁻¹ (= $1/R_{overall} = \dot{q}_{removal}/\{T_{r=o} - T_{cool}\}$) Hence, the contribution of $R_{th,ex,total}$ to $R_{overall}$ is only about 28% (R_{bed}: 41%; $R_{w,int}$: 31%), i.e. the thermal resistances related to the effective heat conduction in the fixed bed and to the convective heat transfer at the internal wall dominate the overall radial heat transfer, as also shown by a typical radial temperature profile depicted in Fig. S14.

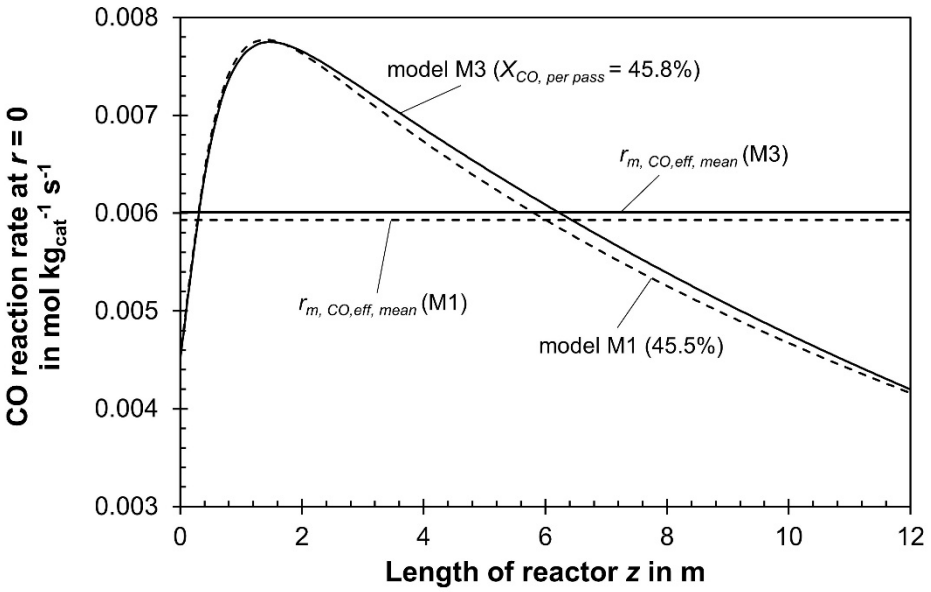

Fig. **S4**: Profiles of reaction rate in the center of a tube of a multi-tubular FT reactor for model 3 (considering Δp_{bed} and change/decline of total molar flow by FT reaction). For comparison, results of model M1 (without Δp_{bed} and without $\Delta \dot{n}_{total}$, i.e. constant u_s, dashed lines) are also shown (C_a = 3; $u_{s,\ z=0}$ (230°C, 30 bar) = 1 m/s; other conditions in Tab. 3). Horizontal lines represent mean values.

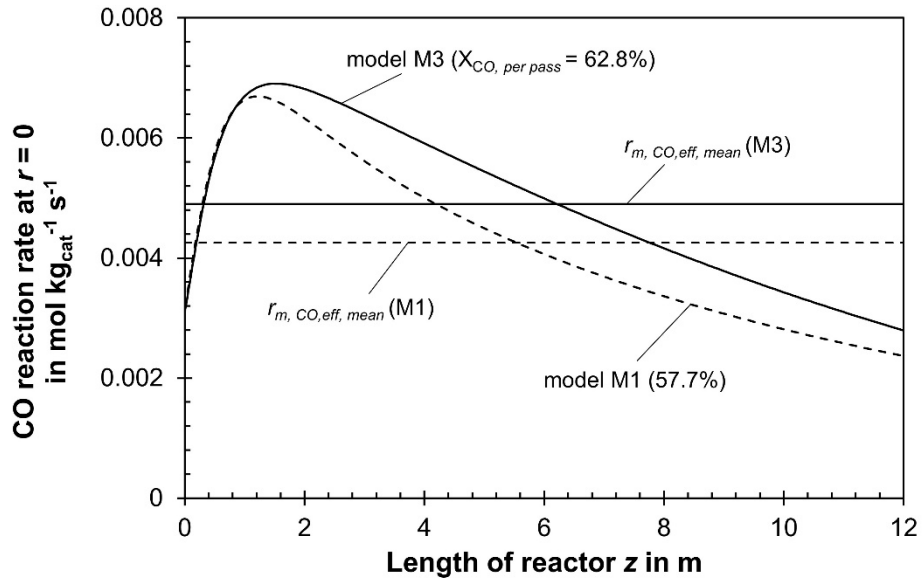

Fig. **S5**: Profiles of reaction rate in the center of a tube of a multi-tubular FT reactor for the model 3 (considering Δp_{bed} and change of the total molar flow). Results for model M1 (without Δp_{bed} and assuming constant u_s) are also shown (C_a = 2; $u_{s,\ z=0}$ (230°C, 30 bar) = 0.5 m/s; other conditions in Tab. 4). Horizontal lines represent mean values. For model M1, the gas velocity is constant and thus also the heat transfer parameters $\alpha_{w,int}$ and λ_{rad}. For M3, $\alpha_{w,int}$ declines along the tubes from 1025 to 877 W m^{-2} K^{-1} and λ_{rad} from 4.4 to 3.4 W m^{-1} K^{-1}, which intensifies the effect of declining gas velocity on deviation of axial profiles of temperature and effective reaction rate.

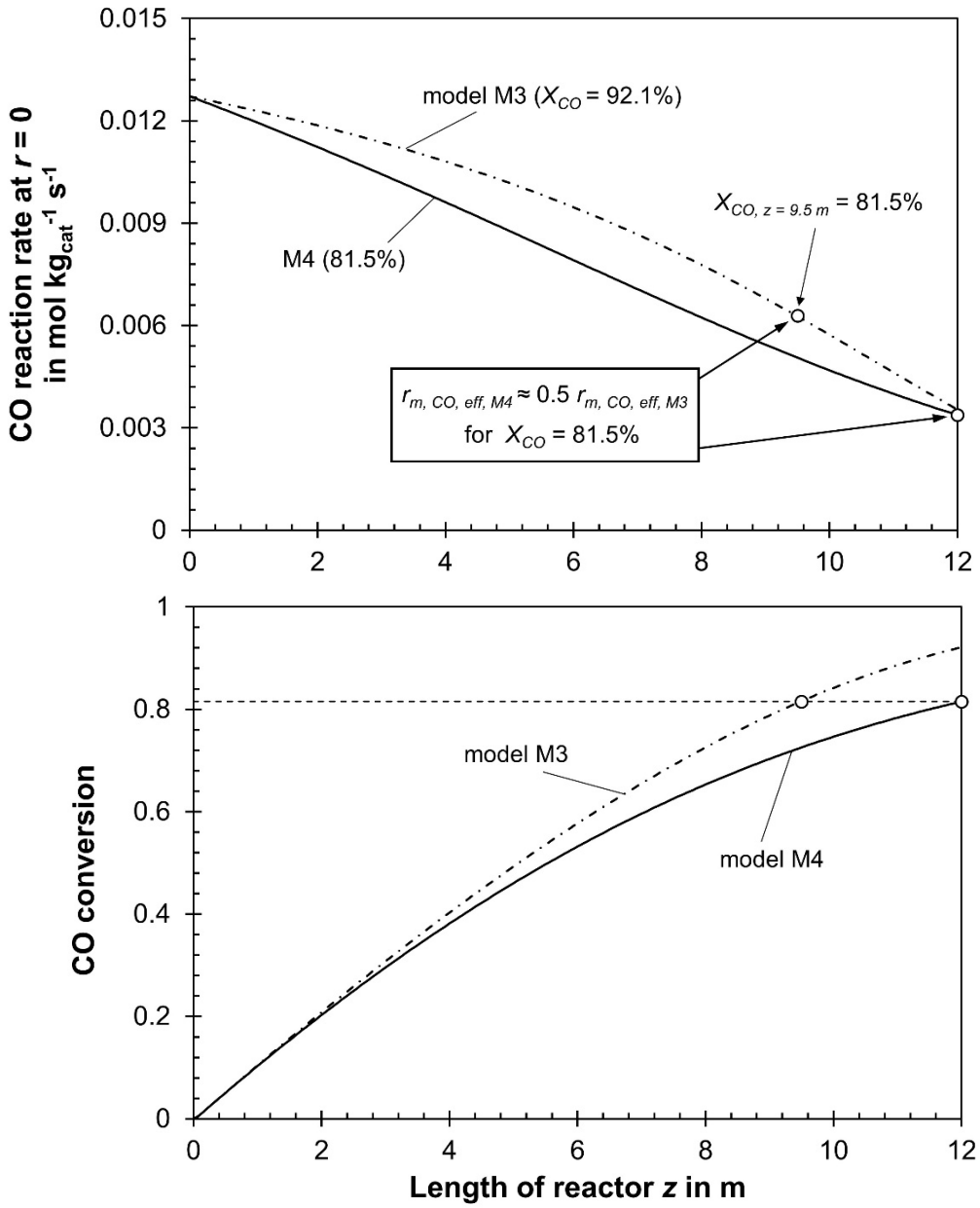

Fig. S6: Profiles of reaction rate of CO conversion at r = 0 (center of tube) (top) and CO conversion (bottom) in an isothermal FT reactor for model M3 (considering Δp_{bed} and change of the total molar flow rate, but not the inhibition by steam/water) and for model M4 (considering also inhibition by steam). Conditions: syngas with only H_2 and CO; C_a = 4; $u_{s,\,z\,=\,0}$ (230°C, 30 bar) = 0.5 m/s; p_{total} = 30 bar; S_{CH_4} = 20%; molar H_2-to-CO ratio = 2.2; 240°C). Inhibition by steam gets strong for z > 4 m, i.e. for a CO conversion above about 40%.

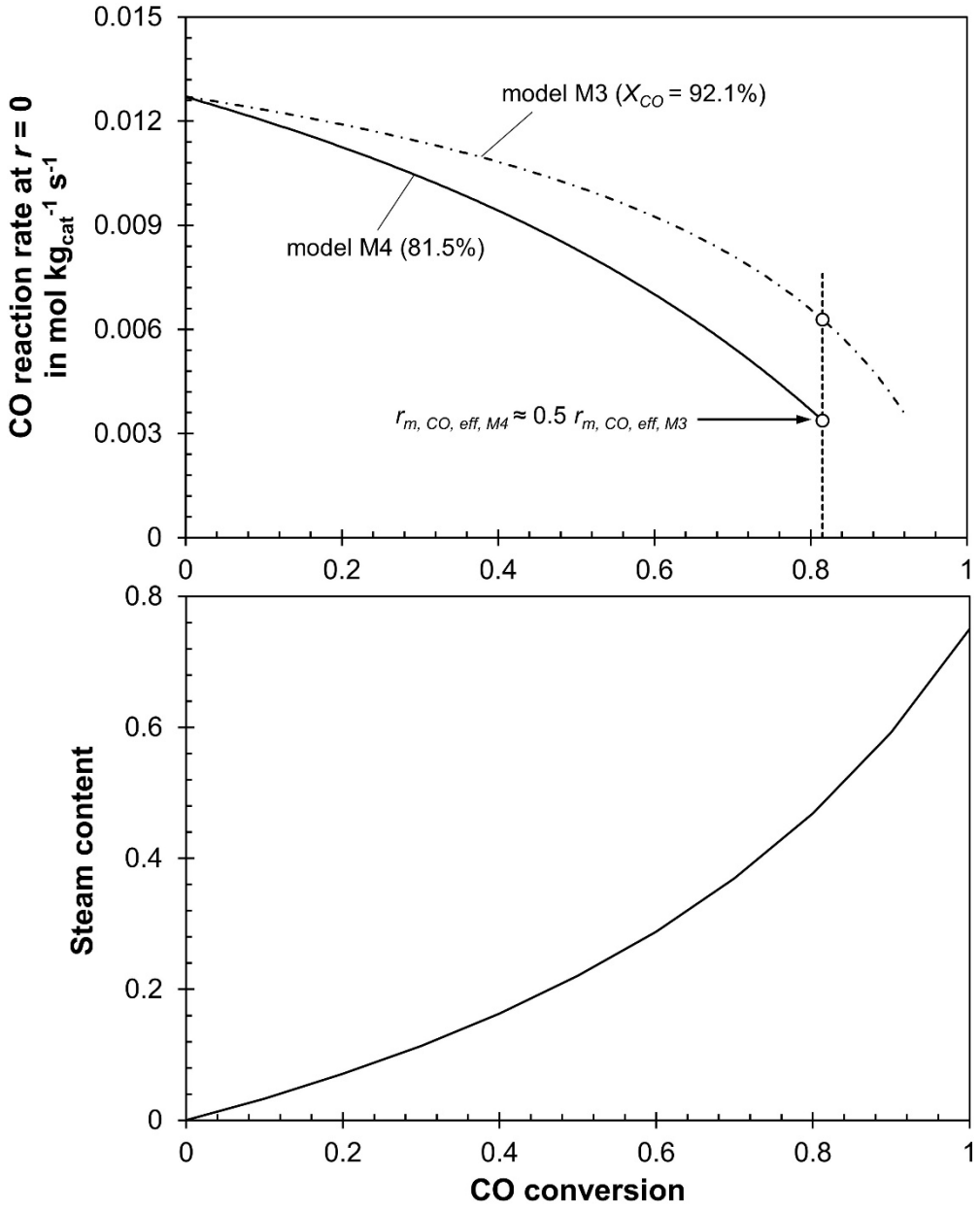

Fig. S7: Influence of CO conversion on the effective reaction rate at r = 0 (center of tube) (top) and steam content (bottom) in an isothermal FT reactor for model M3 (considering Δp_{bed} and change of total molar flow rate, but not inhibition by steam/water) and for model M4 (considering also inhibition by steam). Conditions: Syngas with only H_2 and CO; C_a = 4; $u_{s,\,z=0}$ (230°C, 30 bar) = 0.5 m/s; p_{total} = 30 bar; S_{CH_4} = 20%; molar H_2-to-CO ratio = 2.2; T = 240°C = const. Inhibition by steam gets strong for a CO conversion above about 40%, which corresponds to a volumetric steam content of 18% (about 5 bar).

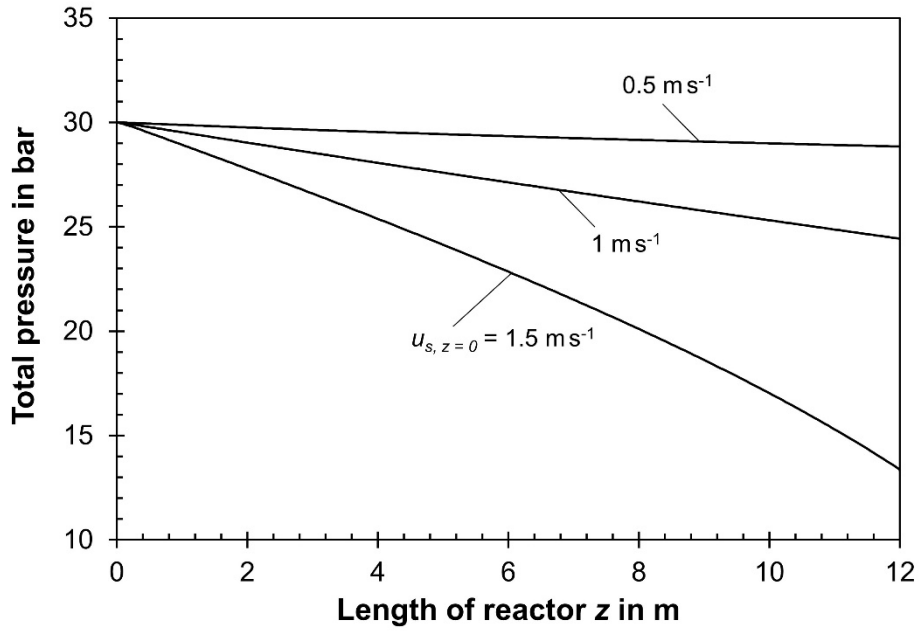

Fig. **S8**: Influence of initial superficial gas velocity $u_{s,\,z=0}$ (at 230°C and 30 bar) on axial profile of total pressure in the tubes of a multi-tubular FT reactor (model M4; C_a = 3; p_{total} = 30 bar; $X_{CO,total}$ = 95%; S_{CH_4} = 20%; H_2-to-CO ratio = 2.2; T_{max} = 240°C).

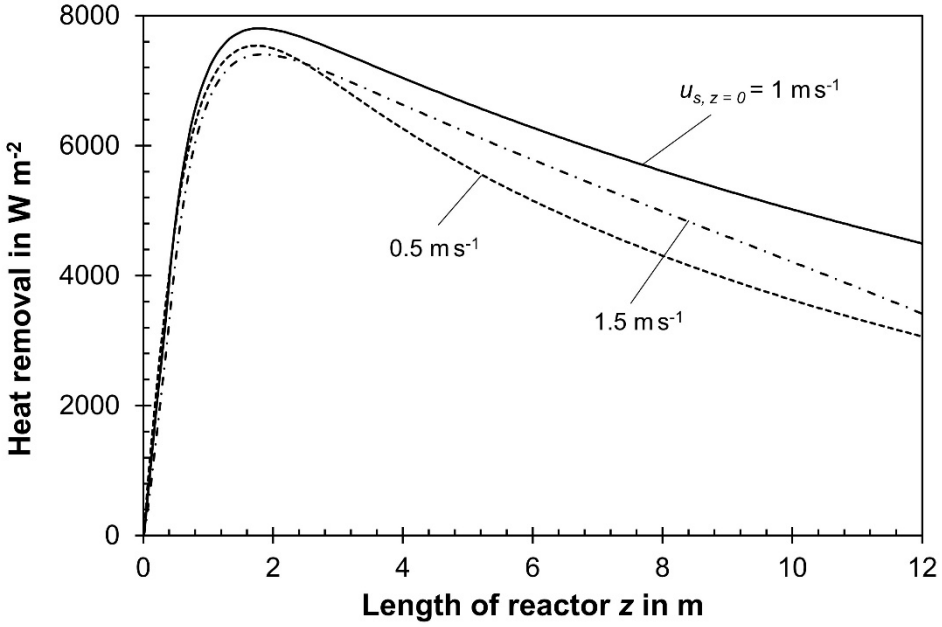

Fig. **S9**: Influence of initial superficial gas velocity $u_{s,\,z=0}$ (at 230°C and 30 bar) on axial profile of rate of heat removal from fixed bed to boiling water in the tubes of a cooled multi-tubular FT reactor. T_{cool} is 213°C for $u_{s,z=0}$ of 0.5 m/s, 223°C (1 m/s), and 227°C (1.5 m/s). Conditions: model M4; C_a = 3; p_{total} = 30 bar; $X_{CO,total}$ = 95%; S_{CH_4} = 20%; molar H_2-to-CO ratio = 2.2; T_{max} = 240°C.

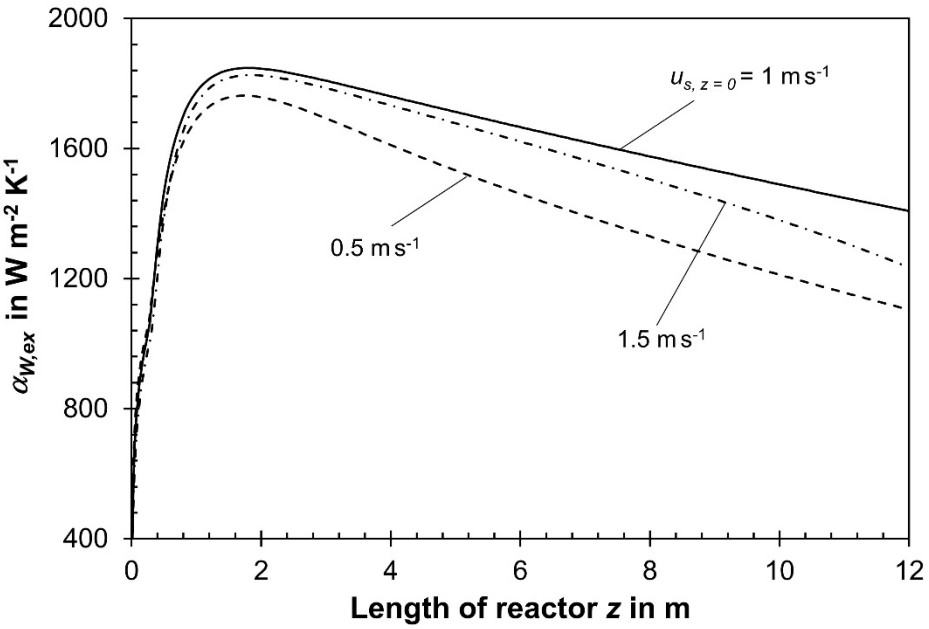

Fig. **S10**: Influence of initial superficial gas velocity $u_{s,\,z\,=\,0}$ (230°C, 30 bar) on axial profile of heat transfer coefficient from tube to boiling water ($\alpha_{w,ex}$) in the tubes of a cooled multi-tubular FT reactor (model M4; C_a = 3; p_{total} = 30 bar; $X_{CO,total}$ = 95%; S_{CH_4} = 20%; molar H_2-to-CO ratio = 2.2; T_{max} = 240°C).

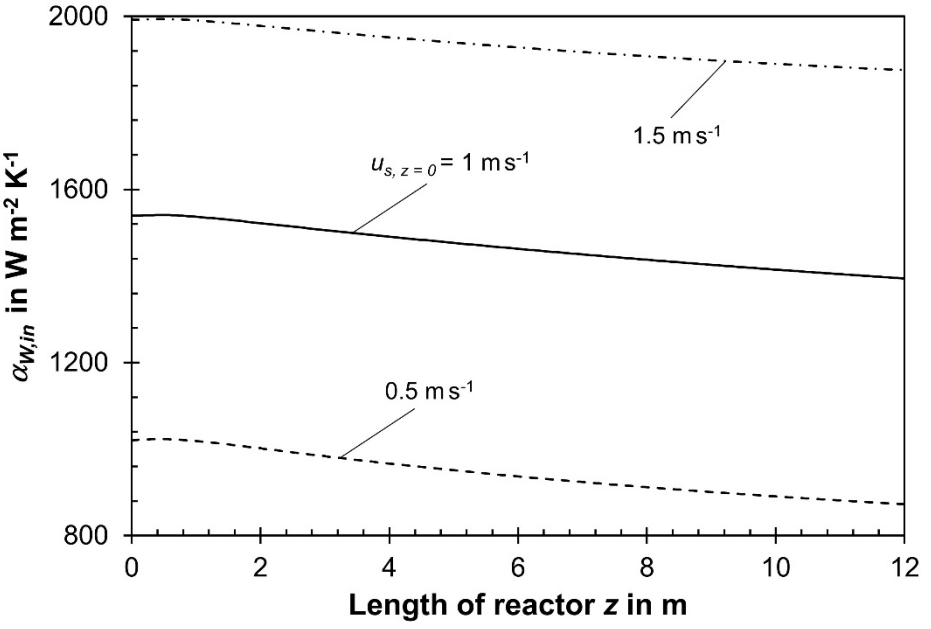

Fig. **S11**: Influence of initial superficial gas velocity $u_{s,\,z\,=\,0}$ (at 230°C and 30 bar) on axial profile of heat transfer coefficient from fixed bed to internal tube wall ($\alpha_{w,int}$) in the tubes of a cooled multi-tubular FT reactor (model M4; C_a = 3; p_{total} = 30 bar; $X_{CO,total}$ = 95%; S_{CH_4} = 20%; molar H_2-to-CO ratio = 2.2; T_{max} = 240°C).

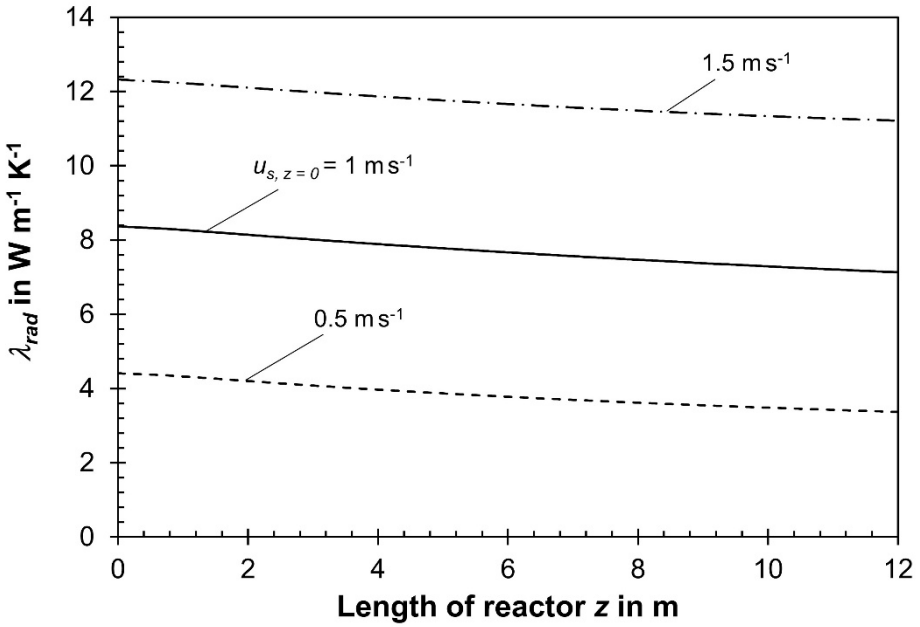

Fig. **S12**: Influence of initial superficial gas velocity $u_{s,\ z\ =\ 0}$ (at 230°C and 30 bar) on axial profile of effective radial thermal conductivity (λ_{rad}) in the fixed bed of the tubes of a cooled multi-tubular FT reactor (model M4; C_a = 3; p_{total} = 30 bar; $X_{CO,total}$ = 95%; S_{CH_4} = 20%; molar H_2-to-CO ratio = 2.2; T_{max} = 240°C).

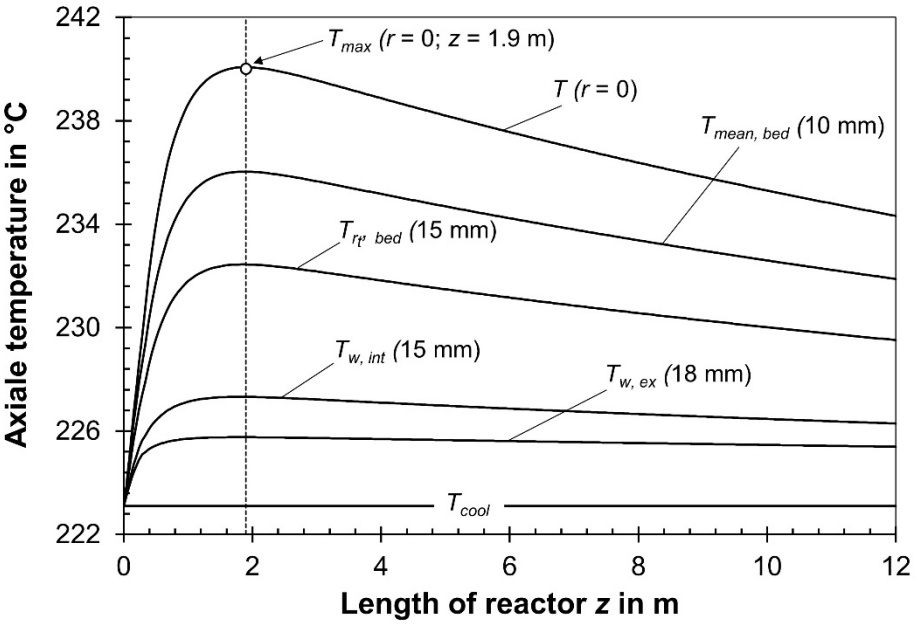

Fig. S13: Axial temperature profiles at different radial positions (model M4; C_a = 3; $u_{s,\ z\ =\ 0}$ (230°C, 30 bar) = 1 m/s; p_{total} = 30 bar; $X_{CO,total}$ = 95%; S_{CH_4} = 20%; molar H_2-to-CO ratio = 2.2; T_{max} = 240°C). For radial profile at z = 1.9 m see Fig. S14.

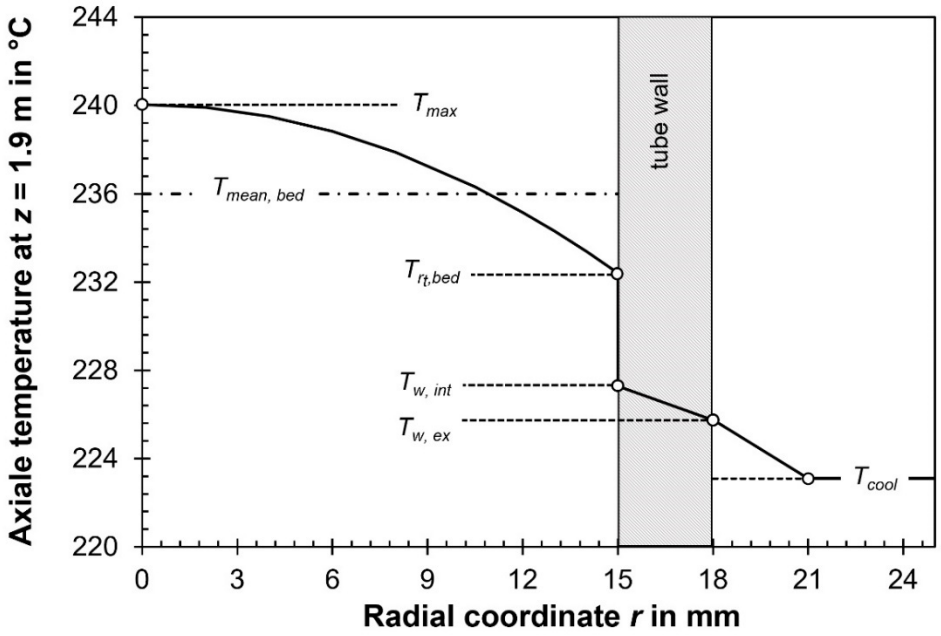

Fig. S14: Radial T-profile at z = 1.9 m, i.e. at the position of the axial temperature maximum, see Fig. S13. Conditions: model M4; C_a = 3; $u_{s,\,z=0}$ (230°C, 30 bar) = 1 m/s; 30 bar; $X_{CO,total}$ = 95%; S_{CH_4} = 20%; molar H_2-to-CO ratio = 2.2; T_{max} = 240°C. The decline of temperature from the external side of the wall (starting at r = 18 mm) into the boiling water is not calculated by the model and only very schematically shown as linear decrease without any real values of radial position.

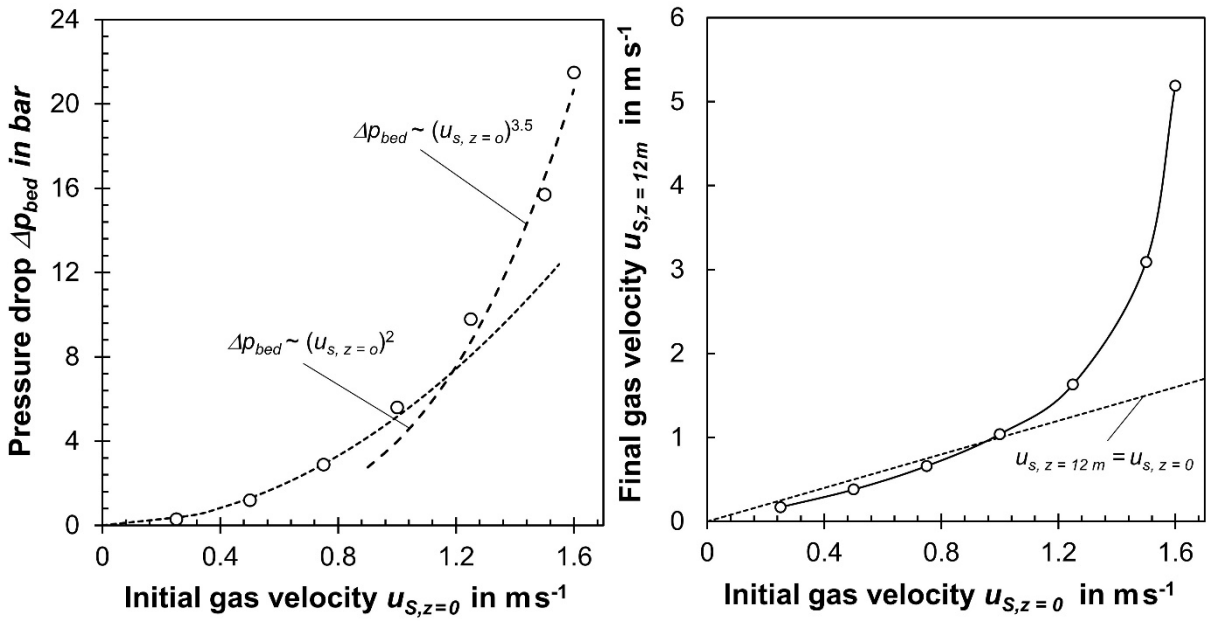

Fig. **S15**: Influence of initial superficial gas velocity $u_{s,\,z=0}$ (230°C, 30 bar) on the pressure drop Δp_{bed} (left) and the final gas velocity $u_{s,\,z=12\,m}$ in the tubes of a cooled multi-tubular FT reactor (right). Conditions: model M4; C_a = 3; p_{total} = 30 bar; $X_{CO,total}$ = 95%; S_{CH_4} = 20%; molar H_2-to-CO ratio = 2.2; T_{max} = 240°C.

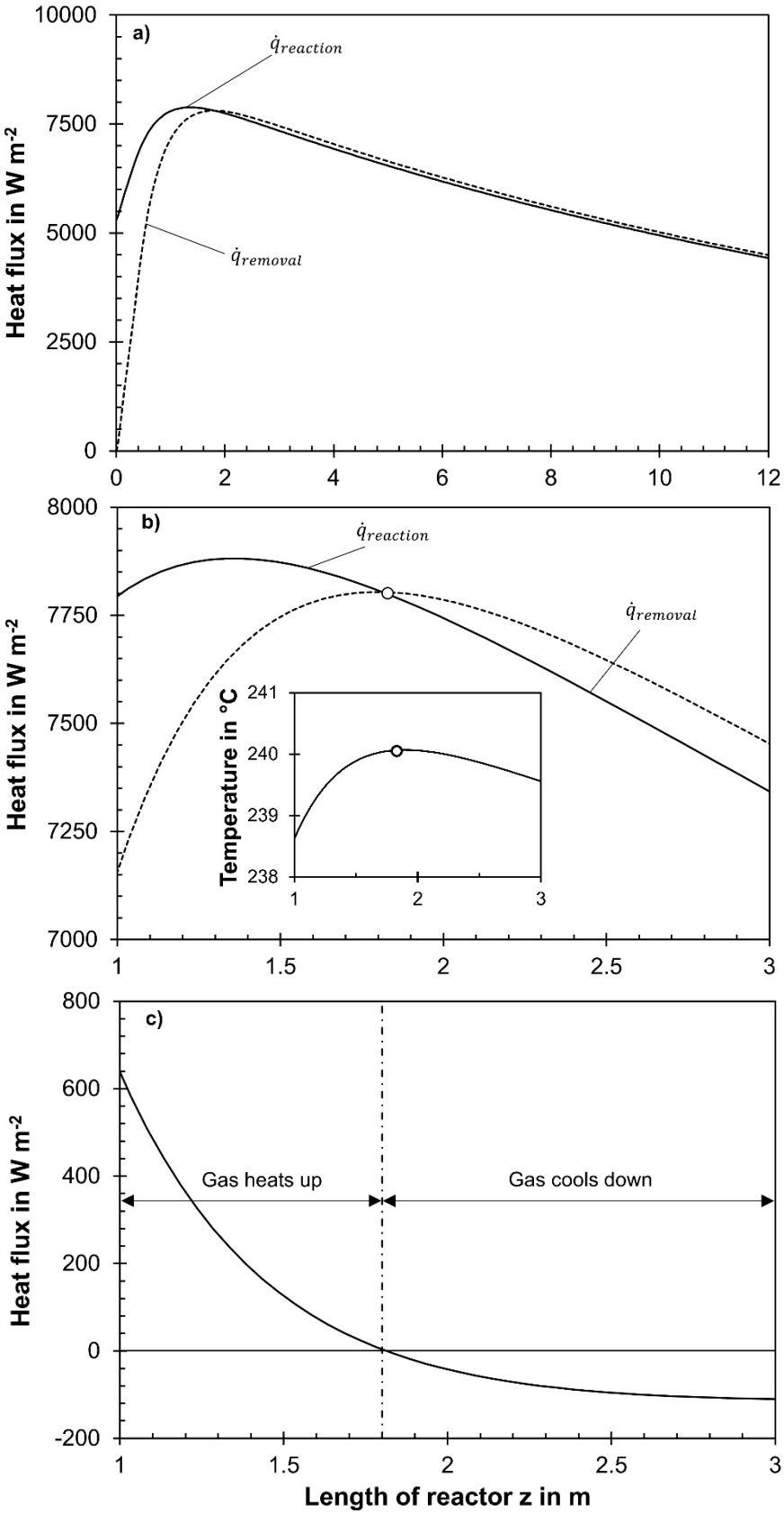

Fig. **S16**: Axial profiles of heat fluxes (W/m^2) in the tubes: a) and b) heat removal and heat production; c) heat flux from/to gas (cooling or heating of gas = heat production minus heat removal) (model M4; C_a = 3; u_s (230°C, 30 bar) = 1 m/s; p_{total} = 30 bar; $X_{CO,total}$ = 95%; S_{CH_4} = 20%; H_2-to-CO ratio = 2.2; T_{max} = 240°C).

A well-known approximation for the maximum (critical) difference between the maximum temperature (center of tubes), here reached at $z \approx 2$ m, and T_{cool} to avoid a reactor runaway is [8]:

$$\Delta T_{crit} = T_{max,ax} - T_{max,cool} = \approx \frac{R\, T_{max,cool}^2}{E_A} \qquad \text{(S19)}$$

$T_{max,ax}$ and $T_{max,cool}$ in Eq. (S19) correspond to the highest values of the axial temperature (center of bed) and the cooling temperature, respectively, to avoid a thermal runaway.

The activation energy can be determined by the Arrhenius plot (Fig. S17), i.e. by ln ($r_{m,CO}$) versus 1/T. The slope leads to $E_{A,intrinsic}$ (if pore diffusion is neglected, i.e. $\eta_{pore} = 1$) = 150 kJ/mol and to $E_{A,eff}$ (effective, i.e. apparent value) = 80 kJ/mol. It should be noted that the values of $E_{A,intrinsic}$ and $E_{A,eff}$ correctly reflect the overall sensitivity of the reaction rate and not only the influence of temperature on the rate constant; the equations of the intrinsic rates of formation of CH_4 and C_{2+}-HCs (Langmuir-Hinshelwood approaches) have two parameters that depend on temperature, the rate constant (k_m) and a parameter for CO adsorption (K); for example, the intrinsic reaction rate of CO leading to C_{2+}-HCs is given by [1]:

$$r_{m,CO,C_{2+}} = C_a\, k_{m,C_{2+}} \frac{c_{H_2}\; c_{CO}}{\left(1 + K_{C_{2+}} c_{CO}\right)^2} \qquad \text{(S20)}$$

The "true" activation energy of $k_{m,C2+}$ is 141 kJ/mol and K_{C2+} (0.047 m^3 mol^{-1} at 240°C) declines with temperature ($K_{C2+} = K_{C2+,0} \exp(-Q/R\,T)$ with Q = -4 kJ/mol). Hence, for a high concentration of CO (typically 140 mol m^{-3} at reactor entrance), $K_{C2+}\, c_{CO} = 6.6 >> 1$, and the "overall" activetion energy $E_{A,intrinsic}$ approaches a value of around 150 kJ/mol (= 141 kJ/mol + 2 x 4 kJ/mol).

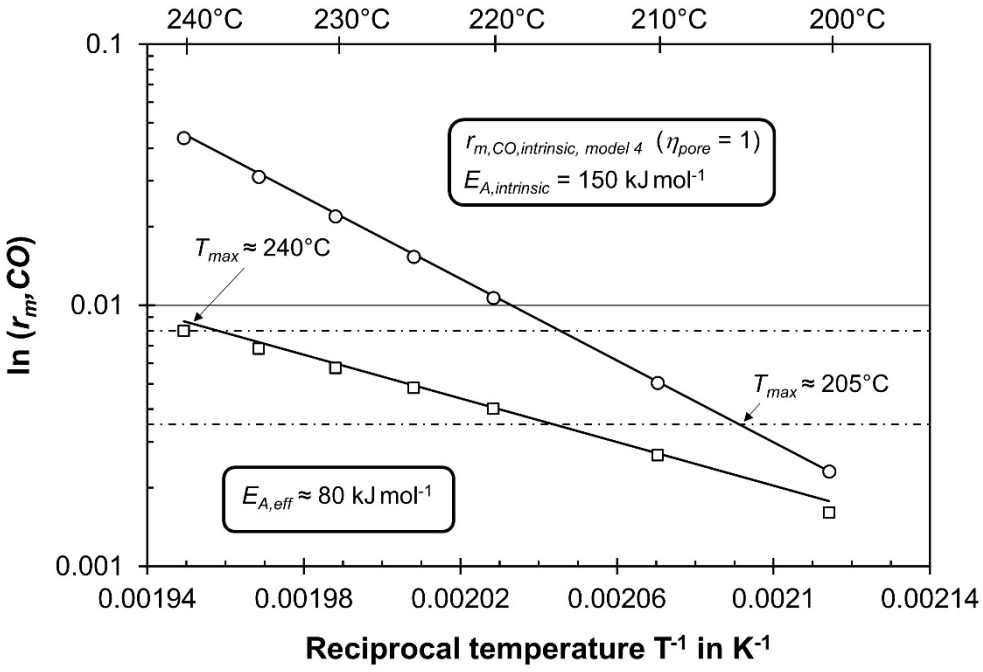

Fig. S17: Arrhenius plot of intrinsic and effective reaction rate of CO conversion at the reactor entrance (model M4; C_a = 3; 19% CO, 42% H_2, 39% CH_4; 30 bar).

The values of ΔT_{crit} according to Eq. (S19) are 13 K (neglecting influence of pore diffusion) and 25 K (pore diffusion correctly considered), if we use a mean value of 490 K for T_{cool}.

Fig. S18 shows the influence of T_{cool} on the maximum axial temperature at r = 0 (left) and on

the difference $T_{max,ax}$ - T_{cool} (right), if pore diffusion is present and also for the hypothetic case of absence of pore diffusion limitations. The calculation was done by model M4 for typical reaction conditions ($u_{s,z=0}$ = 1 m/s; C_a = 3 or 1; syngas: 19% CO, 42% H_2, 39% CH_4; 30 bar). The resulting values of ΔT_{crit} agree very well with the values just given above.

Fig. S18 (lower part) clearly shows that the strong influence of pore diffusion on the effective reaction "helps" with regard to reactor stability and temperature level that can be realized: The ignition temperature, i.e. the critical cooling temperatures estimated graphically as shown in Fig. S18, are very high, 241°C for an activity coefficient C_a of 3 and even 256°C for C_a = 1, which is by far higher than the real cooling temperatures to reach the assumed maximum temperature of 240°C, e.g. 223°C for C_a = 3 and u_s = 1 m/s (see Tab. 8).

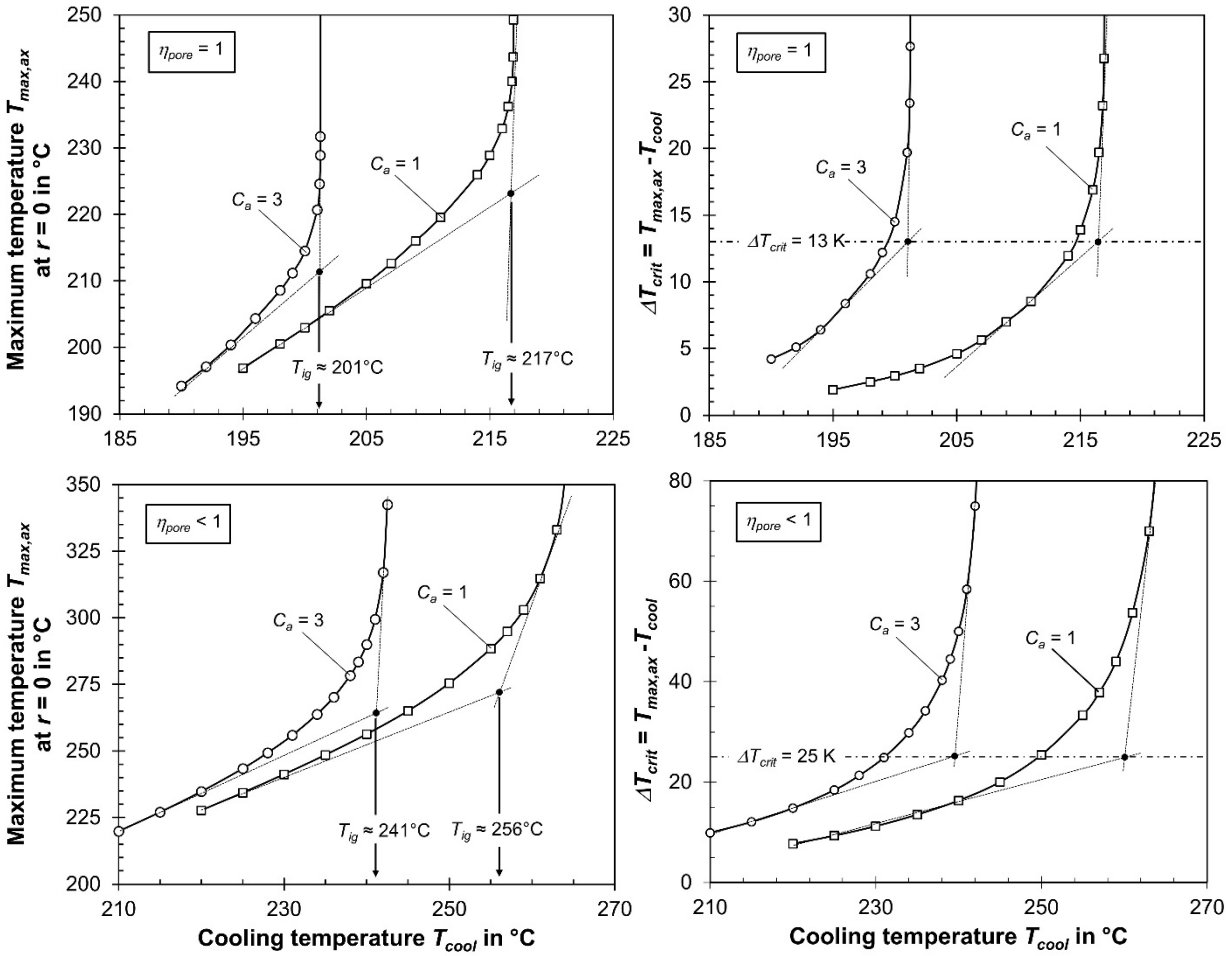

Fig. S18: Influence of T_{cool} on $T_{max,\,ax}$ at r = 0 (left) and on difference $T_{max,ax}$ - T_{cool} (right), if pore diffusion is present and for hypothetic case of absence of pore diffusion limitations (model M4; $u_{s,z=0}$ = 1 m/s; C_a = 3 or 1; 19% CO, 42% H_2, 39% CH_4; 30 bar).It should be mentioned that for very high temperatures (>> 240°C) the model does not accurately account for the then much higher methane selectivity as assumed here (20% related to carbon).

For the hypothetical case of absence of pore diffusion limitations, this is quite different (upper part of Fig. S18): The estimated critical cooling temperatures are now only about 201°C for C_a of 3 and 217°C for C_a = 1, and with ΔT_{crit} of 13 K, we can estimate maximum axial temperatures

of only 215°C for C_a of 3 and 231°C for C_a = 1 (see Tab. 8), which are much lower than the target value of 240°C. To ensure a safe operation, the maximum cooling temperature should be set 5 K below the ignition temperature (T_{ig}). Hence, T_{max} will be even lower at around 205°C for C_a of 3 (see left upper part of Fig. S18). Fig. S17 shows that the intrinsic rate at this temperature is by about 50% lower compared to the effective rate at 240°C, which again underlines the advantage of the influence of pore diffusion for FT fixed bed synthesis, also shown by the results listed in Tab. 8: For C_a = 3 and u_s = 1 m/s, the CO conversion is 44.4% for η_{pore} < 1 and only 28.4% for the hypothetical case of η_{pore} = 1.

Tab. S1: Comparison of different axial distributions of the catalytic activity C_a, simulated by the most "accurate" model M4: Characteristic data of a FT reactor with optimal activity distribution for $C_{a,mean}$ = 3, i.e. $C_{a,initial}$ until T_{max} of 240°C is reached (at z ≈ 2 m) and thereafter a continuous increase of C_a to keep temperature at 240°C (r = 0) and of a two-zone FT reactor for optimal values of activity (C_a) in both zones. For comparison the case of no axial distribution is again also listed. Conditions: $X_{CO,total}$ = 95%; S_{CH_4} = 20%; H_2-to-CO ratio = 2.2; T_{max} = 240°C; $u_{s,z=0}$ = 1 m/s.

$C_{a,mean}$	**C_a in zone 1** (z < 6 m) and **zone 2** (6 m < z < 12 m)[a]		$X_{CO,\ per\ pass}$ in %	T_{cool} in °C	R	**Production of C_{2+}-HCs per tube** in kg_C/h (*improvement compared to const. C_a of 3*)
	$C_{a,1}$	$C_{a,2}$				
3	2.5	3.5	45.7	224.1	2.36	1.55 (+ *4%*)
$C_{a,mean}$	**Optimal distribution of C_a:** $T \approx T_{max}$ = 240°C as soon as T_{max} is reached at $z \approx$ 2 m		$X_{CO,\ per\ pass}$ in %	T_{cool} in °C	R	**Production of C_{2+}-HCs per tube** in kg_C/h (*improvement compared to C_a = 3 = const.*)
	$C_{a,initial}$	$C_{a,max}$				
3[b]	2.23	4	46.8	224.8	2.25	1.60 (+ *8%*)
For comparison: No axial distribution of activity (already listed in the Tab. 8)						
C_a = 3 = constant			44.4	223.1	2.49	1.49 (*0%, base case*)

[a] In both zones, the maximum temperature of 240°C is almost reached.

[b] The limiting value of $C_{a,max}$ = 4 (catalyst with about 40 wt.-% Co) is reached at z = 10.1 m. Thereafter, the temperature slightly decreases to 239°C at z = 12 m.

Tab. S1 shows, that for the given conditions, the optimal axial activity distribution (for $C_{a,mean}$ = 3) leads to a CO conversion of 46.8% and production rate of C_{2+}-HCs per tube of 1.6 kg_C/h. The following (hypothetical) boarder case, which cannot be "beaten" for the given catalyst and particle size (hence $\eta_{pore} \approx 0.2$) is also instructive: A simulation for a constant C_a of 3 and both an axially and radially isothermal fixed bed ($\Delta_R H_i$ was then just zeroized in the model) at T_{max} = 240°C leads to a conversion of 51.2% and a rate of C_{2+}-HCs per tube of 1.82 kg_C/h, which is

406 "only" 14% more compared to the optimal activity distribution and a real cooled multi-tubular
407 FT reactor with an unavoidable axial and radial (see e.g. Fig. S14) temperature profile.

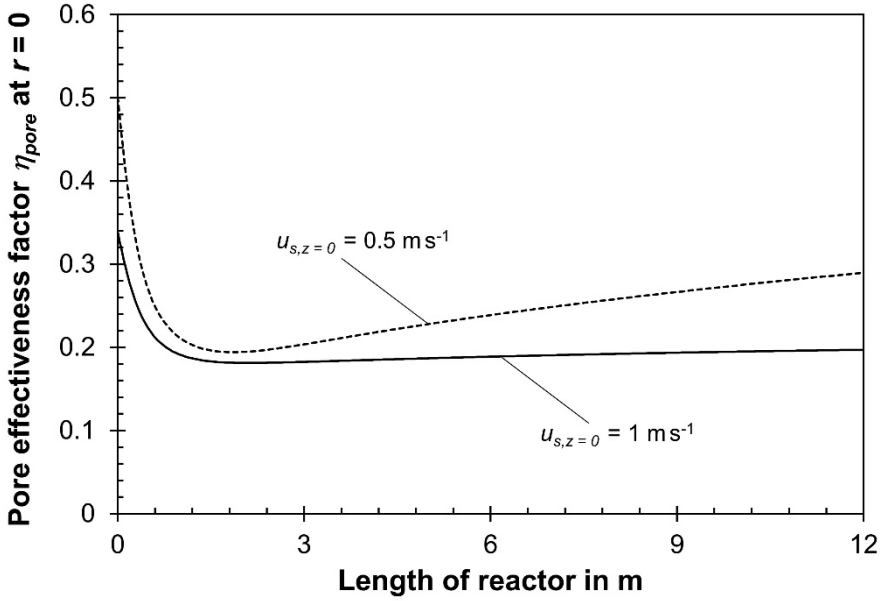

421 **Fig. S19**: Axial profiles of pore effectiveness factor η_{pore} (center of tube) for a superficial gas
422 velocity u_s (230°C, 30 bar) of 0.5 and 1 m/s (model M4; p_{total} = 30 bar; $X_{CO,total}$ =
423 95%; S_{CH_4} = 20%; C_a = 3; H_2-to-CO ratio = 2.2; T_{max} = 240°C; see also Tab. 8). η_{pore}
424 strongly depends on temperature. The temperatures at z = 0 (center of tube; r = 0)
425 are 213°C (u_s = 0.5 m/s) and 223°C (u_s = 1 m/s); at z = 12 m we have 226°C (u_s =
426 0.5 m/s) and 234°C (u_s = 1 m/s), see also Fig. 9. Selected values of factor η_{pore} at
427 different temperatures and the reactor entrance are listed in Tab. S2

428 **Tab. S2**: Values of pore effectiveness factor η_{pore} at different temperatures (reactor entrance,
429 syngas with 20% CO, 44% H_2, and 36% CH_4; C_a = 3; p_{total} = 30 bar).

T in °C	η_{pore}
170	96.8%
180	92.4%
190	83.9%
200	70.3%
210	53.7%
220	38.4%
230	26.8%
240	18.8%

430